Influence of coexisting phases on the surface dilatational viscosity of Langmuir monolayers

Juan M. Lopez,[1] Michael J. Vogel,[2] and Amir H. Hirsa[3]
[1]*Department of Mathematics and Statistics, Arizona State University, Tempe, Arizona 85287, USA*
[2]*School of Chemical and Biomolecular Engineering, Cornell University, Ithaca, New York 14853, USA*
[3]*Department of Mechanical, Aerospace and Nuclear Engineering, Rensselaer Polytechnic Institute, Troy, New York 12180, USA*
(Received 11 February 2004; revised manuscript received 27 April 2004; published 17 November 2004)

Monolayer hydrodynamics are usually described in terms of a Newtonian constitutive relationship. However, this macroscopic view fails to account for small-scale coexisting phase domains, which are generally present in the monolayer and appear to have profound macroscopic effects. Here, we provide direct evidence of these effects, consisting of Brewster angle microscopy images of the monolayer, space- and time-resolved interfacial velocity measurements, and comparisons with predictions based on the Navier-Stokes equations together with the classic model for a Newtonian interface.

DOI: 10.1103/PhysRevE.70.056308 PACS number(s): 47.20.Hw, 68.03.Hj, 47.20.Ma, 83.80.Qr

Surfactant monolayers on the air/water interface are ubiquitous not only in nature [1] and technology [2], but practically every laboratory experiment with a free surface is influenced, if not dominated, by surfactants [3]. In many circumstances, the transport of mass, momentum, and energy can be strongly influenced by the viscoelastic nature of the monolayer-covered interface [4]. This is because only a minuscule amount of surfactant is needed to produce considerable changes in the interfacial properties of aqueous systems. The defining tendency of surfactant molecules is to collect in a monomolecular layer at the gas/liquid interface where they reduce the surface tension. Consequently, surfactants make the interface elastic due to the general decrease in surface tension with increasing surface concentration of the surfactant. In addition, surfactants can impart intrinsic interfacial viscosities representing viscous resistence to shearing and to compression/expansion of the monolayer.

The coupling between a surfactant monolayer on a fluid interface and bulk flow has traditionally been modeled using the Boussinesq-Scriven constitutive relation for a Newtonian interface [5], where the surface stress tensor τ is a linear function of the surface rate-of-deformation tensor $2\mathbf{D}$:

$$\tau = \nabla\sigma + \nabla[(\kappa^s - \mu^s)\mathrm{div}\,\mathbf{u}^s] + 2(\nabla\mu^s)\cdot\mathbf{D} + 2\mu^s\,\mathrm{div}\,\mathbf{D}; \tag{1}$$

$\mathbf{u}^s$ is the surface velocity, div is the surface divergence operator, and ∇ is the surface gradient operator. The three intrinsic interfacial properties, namely (i) thermodynamic (equilibrium) surface tension σ, (ii) surface shear viscosity μ^s, and (iii) surface dilatational viscosity κ^s, are treated as functions of a single state variable: monolayer (surface) concentration c. This model is based on the premise that interfacial stress is due to gradients in the thermodynamic (equilibrium) surface tension and that any departures from equilibrium are due to *dissipative* effects associated with the intrinsic interfacial viscosities. The assumption that departures from thermodynamic surface tension must be dissipative is based on the two-dimensional analog of a single phase fluid and in general may not be applicable to monolayers with coexisting phases.

In contrast to three-dimensional systems in which at a given temperature, saturated liquid and vapor phases coexist only at one pressure, coexistence of different phases in monolayers is common over a wide range of states. Originally inferred from the functional form of the measured equation of state $\sigma(c)$, monolayer phase coexistence has recently been observed directly using microscopic techniques, such as fluorescence microscopy [6] and Brewster angle microscopy (BAM) [7]. In three dimensions, the (shear) viscosity of the two phases is not the same (in the case of water, they differ by two orders of magnitude), and likewise the viscoelastic properties of the interface are not expected to be uniform for a monolayer composed of coexisting phases [8].

Surface tension is well defined in a continuum (macroscopic) sense even when there is coexistence of phases. Being an equilibrium quantity, it is commonly measured quasistatically using a Langmuir trough, and is used successfully in static equilibrium problems, such as predicting the shapes of static menisci and bubbles. Shear viscosity has also been consistently measured by a variety of techniques, all of them implemented at steady state [9,10], and the effects due to coexisting phases are possibly manifested in the long times to reach equilibrium [11]. The situation with dilatational viscosity κ^s is much more complicated; its measurement using techniques with different time scales for the surface strain varies by as much as a factor of 10^5 for a given surfactant [12]. In a compressing or dilating interfacial flow, the time scale for the flow process is usually different from the time scales associated with morphology among the coexisting monolayer phases. Thus, resistance to compression or dilation as predicted using equilibrium surface tension gradients may not be reconciled with the resultant stress. In fact, several different groups [13] have reported measurements of apparent negative surface dilatational viscosity (negative viscosity is physically inconsistent as it violates the second law of thermodynamics) and some have conjectured this anomaly to be due to monolayer phase behavior [14], but it remains a hotly debated issue [15]. In this paper, we provide the first direct evidence supporting this conjecture, consisting of Brewster angle microscopy images of the monolayer along with space- and time-resolved interfacial velocity measure-

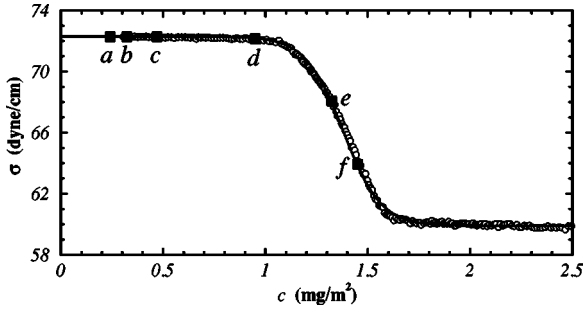

FIG. 1. Equation of state, $\sigma(c)$, for vitamin K_1 (at 22.5 °C), which forms an insoluble monolayer on the surface of water, measured using a Langmuir trough. The open circles are the measurements and the solid line is a curve fit $\sigma=66.1+6.2\tanh[7.5(1-c/1.38)]$; the annotated points $a-f$ correspond to the states presented in the BAM images in Fig. 2.

ments and compared to predictions based on the Navier-Stokes equations with the classic Newtonian interfacial model.

For this study, well-behaved insoluble (Langmuir) monolayers on water have been used. They are well-behaved in the sense that measurements of $\sigma(c)$ during quasistatic compression in a Langmuir trough give essentially identical results to measurements during expansion over a wide range of initial and final concentration. An example of such a monolayer is vitamin K_1 [16]. The measured equation of state for vitamin K_1 is shown in Fig. 1. Predictions of velocity (both on the interface and in the bulk) using the Boussinesq-Scriven surface model for this monolayer coupled to Navier-Stokes equations agree with measurements in steady flows with inertia over a wide range of monolayer concentrations and flow conditions [10,17]. Nevertheless, microscopic images of the interface reveal that this monolayer has rich structure consisting of coexisting phase domains (observable in the $1-1000$ μm range) over a wide range of concentration, as shown in Fig. 2 [18]. Figure 2(a) shows that even at this low concentration ($c=0.24$ mg/m^2), where the surface tension is essentially indistinguishable from that of pure water, coexisting phase domains are clearly visible. These consist of liquid condensed regions with a bright appearance and liquid expanded regions with a relatively dark appearance. The oval-shaped expanded domains seen along the right side of the photograph in Fig. 2(b) are in fact circular and their foreshortening is due to the oblique viewing of the surface at the Brewster angle (53° for the air/water interface). The portion of the area covered by the condensed phase increases monotonically with surface concentration up to a concentration of about 1.5 mg/m^2, above which an essentially uniform coverage by the condensed phase is apparent [Fig. 2(f)].

To study the dynamics of monolayer compression and dilation, we have utilized a new surface dilatational viscometer [19], which uses a periodically driven bulk flow in a cavity to compress/dilate the monolayer. By avoiding the use of barrier-driven monolayer compression/dilation (longitudinal wave surface dilatational viscometer [20]), this flow-driven system permits the monolayer to be compressed and dilated at larger amplitudes and frequencies, and yet still avoids complicated surface deformation problems. This allows

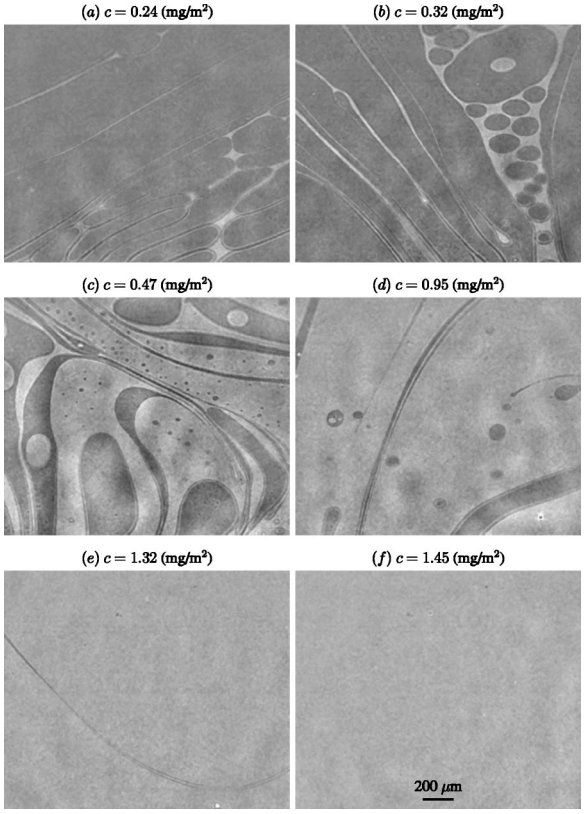

FIG. 2. Brewster angle microscope images of vitamin K_1 monolayer on water. Images were taken during a quasistatic compression (from 0.2 to 1.6 mg/m^2 in about 10 min) in a Langmuir trough, showing coexistence of phases over a wide range of concentrations.

quantification of the monolayer response to a wide range of spatial and temporal gradients and enhances the effects of dilatational viscosity relative to Marangoni stress [19].

The oscillatory driven cavity consists of a rectangular channel $(x,y,z)\in[-1,1]\times[0,1]\times[-\Lambda/2,\Lambda/2]$, where the vertical depth h has been used as the length scale. The walls at $x=\pm1$ and at $z=\pm\Lambda/2$ are stationary, the free surface at $y=1$ is covered by an initially uniform monolayer, and the bottom at $y=0$ oscillates harmonically in its own plane with x velocity given by $\mathrm{Re}\sin(2\pi\mathrm{St}t)$, where Reynolds number $\mathrm{Re}=Uh/\nu$ and Stokes number $\mathrm{St}=\omega h^2/\nu$ (ν is the kinematic viscosity of water, $2\pi/\omega$ is the period of the floor oscillation, and U is its maximum speed). In the experiments, $h=1$ cm and $\Lambda\approx19$. We have shown [21] that over the range of Re and St considered, the flow remains essentially invariant in z, and so all the computations are two-dimensional in (x,y) with velocity (u,v).

The governing equations are the two-dimensional Navier-Stokes equations; in stream-function-vorticity form, where $(u,v)=(\psi_y,-\psi_x)$ and $\eta=-\psi_{xx}-\psi_{yy}$, these are

$$\eta_t+\psi_y\eta_x-\psi_x\eta_y=\eta_{xx}+\eta_{yy}. \tag{2}$$

We take the interface as flat and the contact angle at the air/water/solid contact line as 90° [22]. The tangential stress balance, from Eq. (1), gives

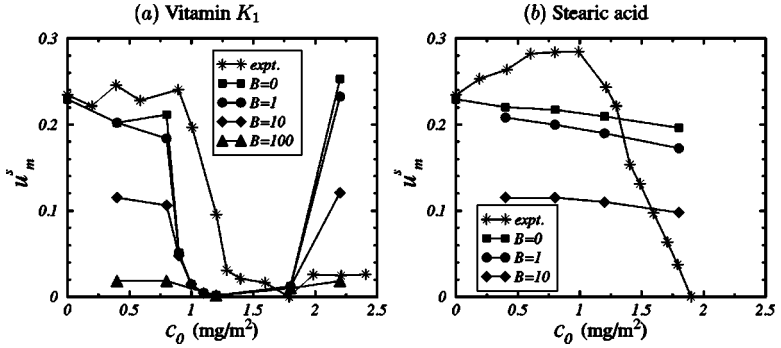

FIG. 3. Measured and computed maximum of x velocity of the surface at the midpoint $(x,y)=(0,1)$, u_m^s (scaled by U), at Re=498 and St=53. The computations are for various $\mathcal{B}$; intersections between the measured and computationed curves give $\mathcal{B}(c)$. Note the apparent negative value of $\mathcal{B}$ (and hence κ^s) over a wide range of c_0 for both monolayers as well as the large values of $\mathcal{B}$ at large c_0.

$$\eta(x,1,t) = -u_y(x,1,t) = -C_a^{-1}\sigma_x - \mathcal{B}u^s_{xx}, \tag{3}$$

where $C_a=\mu\nu/h\sigma_0$ is the capillary number, $\sigma_0=\sigma(0)$, $u^s(x,t)=u(x,1,t)$, and the Boussinesq number $\mathcal{B}=(\kappa^s+\mu^s)/\mu h$ is treated as constant since its functional dependence on c is not known *a priori* (μ is the bulk liquid viscosity). The equation of state, $\sigma(c)$, is measured for the monolayer in question (e.g., see Fig. 1 for vitamin K_1). The vorticity at the interface depends on c, whose distribution is governed by

$$c_t + (cu^s)_x = P_e^{-1}c_{xx}, \tag{4}$$

where $P_e=\nu/D^s$ is the surface Peclet number and D^s is the diffusivity of the monolayer.

The numerical solution of Eqs. (2) and (4) follows that used in [19]. Specifically, a second-order centered finite-difference scheme was used with $n_x=401$ and $n_y=201$ grid points, together with a second-order predictor-corrector scheme for time evolution. The time step, δt, is governed predominantly by $\mathcal{B}$; $\delta t=10^{-7}$ for $\mathcal{B}=0$ and $\delta t=10^{-9}$ for $\mathcal{B}=100$.

The computed maximum value of x velocity at the midpoint of the interface, u_m^s, during each period is plotted in Fig. 3 as a function of monolayer initial (uniform) concentration, c_0, for a range of $\mathcal{B}$. As expected, the response of the monolayers is strongly dependent on their nonlinear equations of state. Data for two different Langmuir monolayers are presented: vitamin K_1 and stearic acid. For both, increased $\mathcal{B}$ generally results in decreased u_m^s, as expected. However, over the range of concentration where the equation of state is steepest (between 0.9 and 1.5 mg/m^2 for vitamin K_1 monolayers), Marangoni stress dominates over surface viscosity effects. Similar behavior was found in earlier computations [19] for this monolayer, but for a set of very different flow conditions (Re=100, St=16).

Measured u_m^s, obtained via boundary-fitted digital particle image velocimetry (DPIV) [23], is also shown for each c_0 in Fig. 3. The sum of the surface viscosities $\mathcal{B}(c)$ can thus be deduced: the point where the measured $u_m^s(c)$ intersects with the computed $u_m^s(c)$ for a given $\mathcal{B}$ determines the value of $\mathcal{B}$ for the corresponding value of c. Figure 3 shows that $\mathcal{B}$ is zero, as expected, for a clean surface (no monolayer). At large monolayer concentrations, $\mathcal{B}$ becomes large. Figure 3(a) shows that for vitamin K_1, at the largest concentration tested ($c_0=2.2$ mg/m^2), $\mathcal{B}$ is about 100. However, the most striking feature of Fig. 3 is the large range of c for which the measured u_m^s is larger than the computed u_m^s for *any* nonnegative value of $\mathcal{B}$, leading to anomalous negative values of $\mathcal{B}$, and hence to negative values of κ^s [24].

The range of c over which the effective $\mathcal{B}$ is negative matches that for which the vitamin K_1 monolayer consists of coexisting phase domains. The same is true for the stearic acid monolayer, which exhibits negative effective $\mathcal{B}$ for c less than about 1.3 mg/m^2. BAM images for stearic acid monolayers at four different concentrations are shown in Fig. 4. From Fig. 4, the upper range of monolayer concentration for which coexisting phase domains are visible is between 1.2 and 1.5 mg/m^2, consistent with the range of c over which apparent negative $\mathcal{B}$ was observed for stearic acid monolayers.

The anomalous behavior was not peculiar to this set of flow conditions (Re=498 and St=53). Comparisons between measurements and computations show the same range of c for which effective $\mathcal{B}$ is negative with the channel driven at a different amplitude (Re=747) as well as a different frequency (St=27), for both vitamin K_1 and stearic acid. Furthermore, experiments in which the surface flow was measured using a very different technique also showed the same range of c for which effective $\mathcal{B}$ is negative for both vitamin K_1 and stearic acid [25]. Thus, the anomalous behavior does not seem to be a relic of the experiment.

The only approximation in the formulation is the use of constant $\mathcal{B}$ for each c_0. This too appears not to be the culprit, for the simple reason that the range of c_0 for which the greatest anomaly is observed (e.g, $1.0<c<1.3$ for vitamin K_1) falls in the region of the equation of state where the Marangoni stress is large and hence spatial gradients of c are

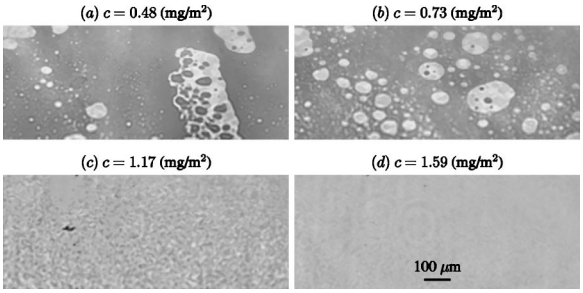

FIG. 4. Brewster angle microscope images of stearic acid monolayer on water. Images were taken during a slow compression in a Langmuir trough. As with the vitamin K monolayer, this monolayer system consists of coexisting phases up to high concentrations.

smallest. Furthermore, even for $\mathcal{B}=0$, where there are no spatial gradients in $\mathcal{B}$, comparisons between computed predictions and experiments show the anomaly.

In closing, we have shown that the classic Newtonian surface model may be inadequate in describing the response of a monolayer-covered interface undergoing dilation or compression for a wide range of monolayer states that consist of coexisting phase domains. For these states, their respective responses to viscous stresses as well as morphological transitions from one phase to another need to be accounted for when the interfacial hydrodynamics drives the system away from equilibrium.

The authors wish to thank Dr. Junqi Ding for assisting with the design and setup of our BAM system. We also thank Professor Michael Dennin and Professor Elizabeth Mann for useful discussions that brought to our attention the importance of coexisting phase domains in Langmuir monolayers and their possible effects on interfacial hydrodynamics. This work was partially supported by the National Science Foundation.

[1] E. J. Bock and N. M. Frew, J. Geophys. Res., [Oceans] **98**, 14 599 (1993); J. B. Grotberg, Annu. Rev. Fluid Mech. **26**, 529 (1994); X. N. Liu and J. H. Duncan, Nature (London) **421**, 520 (2003).

[2] A. M. Schwartz, J. Perry, and J. Berch, *Surface Active Agents and Detergents* (Krieger, Huntington, NY, 1977). B. S. Gallardo *et al.*, Science **283**, 57 (1999); V. X. Nguyen and K. J. Stebe, Phys. Rev. Lett. **88**, 164501 (2002); V. Truskett and K. J. Stebe, Langmuir **19**, 8271 (2003).

[3] J. C. Scott, J. Fluid Mech. **69**, 339 (1975); A. Hirsa and W. W. Willmarth, *ibid.* **259**, 25 (1994).

[4] J. C. R. Hunt, in *Gas Transfer at Water Surfaces*, edited by W. Brutsaert and G. H. Jurka (Reidel, Dordrecht, 1984), pp. 67–82.

[5] J. Boussinesq, C. R. Hebd. Seances Acad. Sci. **156**, 983 (1913); L. E. Scriven, Chem. Eng. Sci. **12**, 98 (1960); J. C. Slattery, *Interfacial Transport Phenomena* (Springer, Berlin, 1990); D. A. Edwards, H. Brenner, and D. T. Wasan, *Interfacial Transport Processes and Rheology* (Butterworth-Heinemann, Boston, 1991).

[6] H. M. McConnell, Annu. Rev. Phys. Chem. **42**, 171 (1991).

[7] S. Henon and J. Meunier, Rev. Sci. Instrum. **62**, 936 (1991).

[8] J. Ding, H. E. Warriner, and J. A. Zasadzinski, Phys. Rev. Lett. **88**, 168102 (2002); J. Ignes-Mullol and D. K. Schwartz, Langmuir **17**, 3017 (2001).

[9] R. J. Mannheimer and R. S. Schechter, J. Colloid Interface Sci. **32**, 195 (1970); T.-S. Jiang, J.-D. Chen, and J. C. Slattery, *ibid.* **96**, 7 (1983).

[10] A. H. Hirsa, J. M. Lopez, and R. Miraghaie, J. Fluid Mech. **470**, 135 (2002).

[11] J. M. Lopez, R. Miraghaie, and A. H. Hirsa, J. Colloid Interface Sci. **248**, 103 (2002).

[12] R. L. Kao, *et al.*, J. Colloid Interface Sci. **148**, 247 (1992).

[13] S. K. Peace and R. W. Richards, Polymer **37**, 4945 (1996); D. Sharp and J. C. Earnshaw, J. Chem. Phys. **107**, 7493 (1997); D. Sharp and J. Eastoe, Langmuir **12**, 2303 (1996); S. K. Peace and R. W. Richards, *ibid.* **14**, 667 (1998); F. Monroy, J. Giermanska-Kahn, and D. Langevin, Colloids Surf., A **143**, 251 (1998); P. He *et al.* , *ibid.* **201**, 265 (2002); F. Monroy *et al.*, J. Phys. Chem. B **106**, 5636 (2002).

[14] J. Giermanska-Kahn, F. Monroy, and D. Langevin, Phys. Rev. E **60**, 7163 (1999); F. Monroy, J. Giermanska-Kahn, and D. Langevin, J. Non-Equil. Thermodyn. **25**, 279 (2000).

[15] D. M. A. Buzza *et al.*, J. Chem. Phys. **109**, 5008 (1998); B. A. Noskov and G. Loglio, Colloids Surf., A **143**, 167 (1998); M. G. Munoz *et al.*, Langmuir **19**, 2147 (2003).

[16] G. L. Gaines, *Insoluble Monolayers at Liquid-Gas Interfaces* (Interscience, New York, 1966); G. Weitzel, A.-M. Fretzdorff, and S. Heller, Hoppe Seyler's Z. Physiol. Chem. **303**, 14 (1956).

[17] A. H. Hirsa, J. M. Lopez, and R. Miraghaie, J. Fluid Mech. **443**, 271 (2001).

[18] Our BAM system uses a frequency-doubled (532 nm) Nd:YAG laser with dual head (New Wave Research, Solo-I). The laser output is directed at an incidence angle of 53° (Brewster angle for air/water interface) from the normal. The beam is passed through a half waveplate (Thorlabs, WPH05M-514) to rotate the polarization to *p*-polarized light, and subsequently a Glan-laser polarizer (Newport, 10GL08AR.14) removes any non-*p*-polarized light. The reflected beam is received using a zoom lens system (Thales-Optem, 70XL, with a $2\times$TV tube) mounted on a CCD camera (Texas Instruments, 1134P).

[19] J. M. Lopez and A. H. Hirsa, J. Colloid Interface Sci. **242**, 1 (2001).

[20] L. Ting *et al.*, J. Colloid Interface Sci. **102**, 248 (1984).

[21] M. J. Vogel, A. H. Hirsa, and J. M. Lopez, J. Fluid Mech. **478**, 197 (2003).

[22] The contact line is fixed by depositing a nonwetting paraffin film on the top surface of the vertical walls. In our experiments, the Froude number, $\mathrm{Fr}=U^2/(gh)\approx 10^{-2}$, and measurements confirm that the interface remains essentially flat [21].

[23] The oscillatory driven cavity is described in [21]. The interfacial velocity was measured using boundary-fitted DPIV [A. H. Hirsa *et al.*, Exp. Fluids **31**, 127 (2001)] with a 180 μm spatial resolution, and the procedure for spreading monolayers and the commercial sources of monolayer-forming materials are described in; M. J. Vogel and A. H. Hirsa, J. Fluid Mech. **472**, 283 (2002). The seeding particles used for the DPIV measurements were 3 μm polystyrene particles stabilized with surface-bound sulfate groups (Aldrich, 45941-0). Water preparation and particle cleaning procedure are described in [17].

[24] The surface shear viscosity for vitamin K_1 has been measured independently, using a deep-channel surface viscometer, and found to be zero for $c<1.6\ \mathrm{mg/m^2}$ [17].

[25] Surface flow was independently measured, without DPIV particles, by placing hydrophobic particles (PTFE, with a mean

diameter of 100 μm, Aldrich 46811-8) on the surface and measuring their range of motion in the x direction. This approach is fundamentally different from the DPIV technique; in DPIV, the seeding particles are fully wetted and generally not in contact with the monolayer, but here the particles are essentially nonwetting and in intimate contact with the monolayer. Additional details on the tracer-particle technique are in M. J. Vogel, Ph.D. thesis, Rensselaer Polytechnic Institute (2002).